

## Cryostatic Micro-CT Imaging of Transient Processes

Steven M. Jorgensen<sup>\*a</sup>, Basil Blank<sup>\*\*b</sup>, Erik L. Ritman<sup>\*a</sup>

<sup>a</sup>Department Physiology and Biophysics, Alfred Bldg. 2-409, Mayo Clinic, 200 First Street SW, Rochester, MN 55905; <sup>b</sup>Advanced Design Consulting, Inc., Lansing, NY 14882

### ABSTRACT

A double walled copper vessel, 32cc in volume, was fabricated for micro-CT scanning tissue specimens maintained at cryogenic temperature. The space between the two nested vessels was evacuated and in two opposing sides of the vessel the copper has been replaced by beryllium foil. Nitrogen gas, boiling off liquid nitrogen, is injected continuously into the top of the chamber during the scanning process. Just prior to venting from the vessel the gas is heated and directed through a narrow gap over the outside of the beryllium "windows" so as to maintain the beryllium "windows" frost-free. A temperature detector within the chamber is used to control the rate of inflow of the nitrogen gas. The frozen specimen is attached to a small horizontal platform on top of a vertical stainless steel pin which exits the base of the vessel through a closely fitting hole and is attached to the computer-controlled rotating stage under the vessel. The vessel and rotation-stage assembly is mounted on a computer-controlled horizontal translation stage which can move the specimen out of the x-ray beam, from time to time, for x-ray beam calibration purposes.

The purpose of this arrangement is to permit scanning of specimens that:

1) either cannot be "fixed" (e.g., with formalin) because of biomolecular analyses which are incompatible with prior fixation or, 2) are "snap"-frozen during a transient process, such as the accumulation and/or washout of radiopaque indicators distributed in microvascular or extravascular compartments, which lasts only seconds and hence is too fast for normal micro-CT methods to capture.

Keywords: X-ray, imaging, three-dimensional, contrast, freezing

### 1. INTRODUCTION

Micro-CT is used to quantitate the three dimensional micro-architecture of tissues such as bone,<sup>1</sup> and the branching geometry of vascular trees in either, whole rodent organs, or biopsies from larger animals or humans.<sup>2</sup> A fundamental problem is that micro-CT scans cannot be performed sufficiently rapidly (i.e., scan completed in seconds) to either capture transient processes such as the progressive build-up and washout of indicators in various physiological compartments in organs, or for specimens that must be scanned fresh (i.e., not fixed so as to not preclude certain subsequent analyses such as immunohistochemistry) and would therefore be liable to degrade and distort during scanning procedure lasting many minutes or hours. The relatively long duration of micro-CT scans results from the fact that in order to maintain an adequate CT image signal-to-noise ratio, the number of x-ray photons needed per voxel is essentially invariant with their size.<sup>3</sup> Consequently, the x-ray exposure, per unit area of the specimen, increases roughly in proportion to the cube of the voxel side-dimension. In addition, the need for near monochromatic x-rays<sup>4</sup> reduces the x-ray flux so that very rapid delivery of the x-ray photons may even be beyond the capability of synchrotron-based micro-CT scanners to overcome.

In order to partially circumvent this limitation we have built a "cryostatic" method of x-ray micro-CT scanning. This method allows us to harvest an in vivo organ at the precise time at which the transient process, such as an indicator dilution process, is at its desired state and then drop the organ into a fluid at cryogenic temperature in order to literally freeze the process in place. If the organ is maintained in this frozen state, and is not allowed to accumulate frost or condensation, the micro-CT scan can proceed over the relatively long period of time needed to acquire the needed x-ray exposure at each angle of view. Moreover, if desired, a time-series of a transient event can be acquired either by harvesting the organ from different animals, (especially in genetically identical mice or rats), each being harvested at a sequential time during the dynamic process or by repeated biopsies of the same organ in a large animal. Although the specimen could be split in half, so that one half could be scanned in a fixed state and the other half subjected to the histological or other analysis, there are reasons to want the micro-anatomic information and tissue analysis in exactly the same location of the specimen. Indeed, the tissue analysis might need to be performed in locations suggested by the micro-anatomic information derived from the micro-CT 3D image.

## 2. METHODS

### 2.1 The Micro-CT Scanner (Figure 1)

The scanner has been described in detail elsewhere<sup>5</sup> so this description is limited to details relevant to this particular application. A spectroscopy x-ray source with the long fine focus geometry and a silver anode, and a paladium, 100  $\mu\text{m}$  thick, foil filter is operated at 50 keV peak (so that 25 keV x-ray photons predominate) illuminates a 1-3  $\text{cm}^3$  specimen positioned approximately one-half meter from the x-ray source. The specimen is positioned as close as possible to the CsI (Tl) crystal plate (0.5 mm thick) which converts the x-ray shadow to a light image. This light image is then projected with a flat field optical lens ( $f/2.8$ , magnification X 1 to X 4) onto a CCD array (1024 x 1024 square pixels, each 24  $\mu\text{m}$  on a side) which is Peltier cooled to  $-40^\circ\text{C}$ . The specimen is positioned on a small horizontal platform on top of a vertical stainless steel shaft which is attached to a rotating stage (Newport, RTN 120 PP) and it in turn is positioned on a translation stage (Newport, UTM 50 PP.1) which can move the specimen in and out of the field-of-view for calibration purposes. The spatial resolution of the scanner is 20 line pairs/mm at x1 optical magnification and 48 line pairs/mm at x 4 optical magnification at 10% signal modulation, which results in the ability to detect 10  $\mu\text{m}$  diameter glass microspheres.<sup>6</sup>

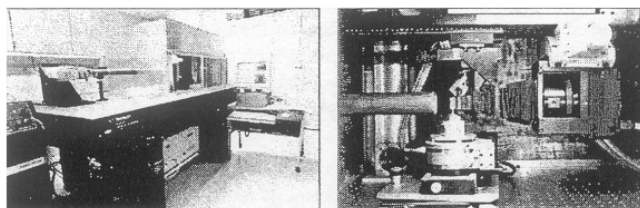


Figure 1 - Photographs of our in-house micro-CT scanners. Left panel: scanner is surrounded by a lead-lined enclosure, which sits on a floating table. The x-ray source (to left of enclosure) is connected to the enclosure via a lead-lined tube. Right panel: details of scanner itself, from left-to-right, the lead-lined tube through which the x-ray beam passes, the specimen (not in the cryogenic vessel, which is not shown in this figure) on its stage "tower" and on the right the x-ray imaging system with the cooled CCD camera on the far right. (Reproduced with permission from Ref. 5)

### 2.2 The "Cryostatic" Vessel (Figures 2 and 3)

A double walled copper vessel, 32 cc in volume, was fabricated for scanning tissue specimens maintained at cryogenic temperatures. The copper walls are 2 mm thick and 6 mm space between the two nested vessels is vacuum brazed and was evacuated and maintained at  $10^{-6}$  torr by a SAES ST 172 getter material,<sup>7</sup> which is a mixture of ZR and ST 707 alloy (ZR-V-FE). This alloy has high diffusivity, large surface area and high porosity. This material continuously scavenges molecules released into the evacuated space, thereby removing the need for continuous mechanical evacuation of the space. The two opposing flat sides of the vessel have been replaced by a high purity IF1 helium-tight beryllium foil, 127  $\mu\text{m}$  thick and 23 mm high x 55 mm wide. This area is wide enough to allow the specimen to be positioned in one half of the window so that the adjacent half can occasionally be translated into the x-ray beam so as to provide the "incident beam" exposure data needed for the tomographic reconstruction process.

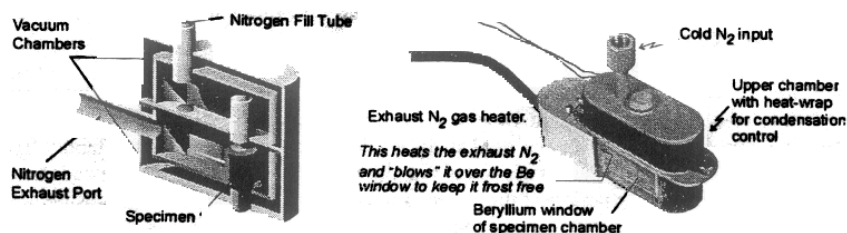


Figure 2 - Schematic of the cryogenic vessel (left) and photo of vessel (right). The specimen is enclosed in a double walled copper vessel (the walls separated by a vacuum) which is immersed in cold nitrogen gas that has 'boiled' off a liquid nitrogen source. The x-ray beam passes through opposing beryllium windows in the vessels. A small diameter, stainless steel rod connects the specimen to the rotational stage. The continuous flow of dry, warmed, nitrogen gas prevents moisture condensation at the point where the outflow of nitrogen flows over the outer beryllium windows.

Nitrogen gas boiling off the liquid nitrogen is vented, via a computer-controlled valve (Tescom) continuously into the top of the chamber during the scanning process. As the gas exits from the chamber it is heated to 30°C and then vented through a narrow gap on one side of the outside of the beryllium "windows". This maintains the windows free of condensation and/or frost. The specimen is attached to a small horizontal platform on top of a vertical stainless steel pin which exits the base of the vessel through a closely fitting hole and is attached to the computer-controlled rotating stage under the vessel.

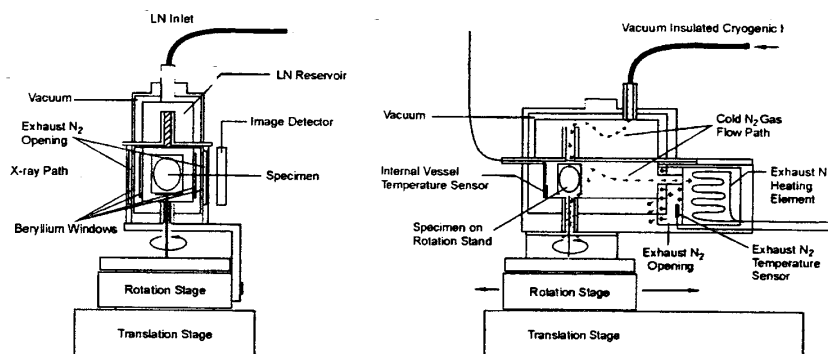


Figure 3 - Left panel is view of vessel at along the x-ray beam and the right panel is view at right angles to the x-ray beam.

### 2.2.1 The Control of the Temperature within the cryogenic vessel during the scan (Figure 4).

A Resistive Temperature Detector (RTD) within the chamber is used to control the rate of inflow of the cold nitrogen gas so as to maintain the specimen temperature within  $\pm 1^\circ\text{C}$  of the desired chamber temperature. The key to this is the Tescom valve which is controlled with a separate source of dry nitrogen pressure at room temperature. The flow from this source is computer-controlled, servoing on the temperature in the chamber. A second RTD monitors the temperature of the exit gas, controlling the heating element duty cycle time to maintain the desired set point ( $\sim 30^\circ\text{C}$ ).

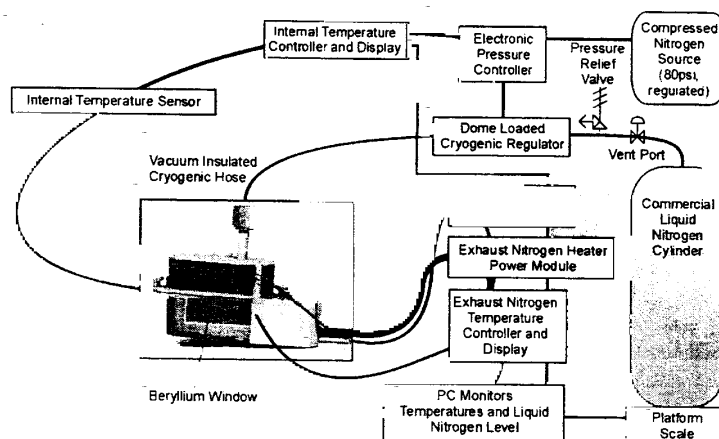


Figure 4 - Schematic of the cold nitrogen delivery and control system. The key is the valve controlling release of liquid nitrogen boil-off. It is controlled by a computer which servoing on the signal from temperature sensor in the scanning chamber.

### 2.3. Specimen preparation

One purpose of the scan is to establish the 3D spatial distribution of an indicator in some physiological space (e.g., the vascular tree, bile ducts, renal tubules or extravascular space). The animal is anesthetized, the organ of interest surgically exposed and the appropriate injection of the contrast agent (e.g., iodinated non ionic contrast agent for intravascular,<sup>8</sup> extravascular or renal tubular<sup>9</sup> opacification and cholegrafen for bile duct<sup>10</sup> opacification) is performed. After the desired interval of time (seconds) the arteries, veins and other anatomic connections between the organ and the rest of the body (e.g., vascular pedicle, ureter, common bile duct) are clamped.

Another purpose of the cryogenic scan is to retain organ "freshness" suitable for subsequent biomolecular analysis. Thus, a lung can be isolated, frozen and scanned. After this, it can be ground-up or sliced for tests requiring fresh frozen specimens. In the case of the lung a deceased mouse was intubated, its lung inflated to 5 mmHg pressure, surgically removed and frozen in the acetone-dry ice slurry. As soon as the organ or biopsy is harvested it is dropped into a small plastic container, which is filled with cold acetone and suspended in an acetone-dry ice slurry. Once frozen it is stored at  $-80^{\circ}\text{C}$  in a freezer until it is scanned.

### 2.3.1 Ancillary Preparation of the Specimens

After the specimen has been successfully scanned it will be processed for the desired histological and/or analytic analysis. This may involve making thin frozen sections or homogenizing the specimen and isolating the desired tissue component.

### 2.4 3D Image Reconstruction and Display

The scan generally consists of 360 x-ray images obtained at one degree angle interval around 360 degrees. These projection images ( $I[x,y]$ , where  $x$  and  $y$  are spatial location of pixel within the CCD array) are then corrected for "black level" (i.e., no x-ray) bias ( $I_b(x,y)$ ) and "white level" (i.e., incident beam,  $I_0(x,y)$ ) so that the resulting x-ray intensity measurement at each pixel is converted to a "density" measurement  $\mu\chi = \log(I_0 - I_b) - \log(I - I_b)$ , in which  $\mu$  is attenuation coefficient of the tissues along path length  $\chi$  of the x-ray beam through the specimen. We then perform a modified Feldkamp cone beam tomographic image reconstruction from these projection data.<sup>11</sup> Display of the stack of tomographic images and their subsequent analyses is performed using the Analyze<sup>TM</sup> software package.<sup>12</sup>

## 3. RESULTS

### 3.1 Temperature Control (Figure 5)

This representative sequence of vessel temperature shows that the temperature does not vary more than  $\pm 1^{\circ}\text{C}$  and that, in this example, it is at  $-18^{\circ}\text{C}$ . The weight of the liquid nitrogen tank is monitored continuously indicating rate of use (usually 2.2 L of liquid nitrogen per hour) so that adequate supply of LN can be predicted for the successful completion of a scan.

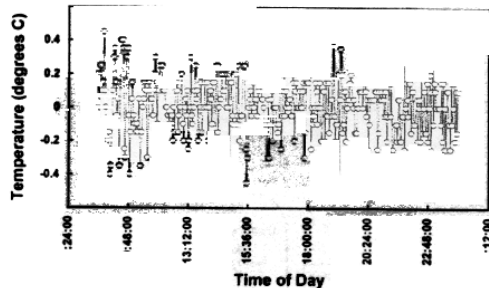


Figure 5 - Temperature trace shows that over a continuous period of 15 hours the temperature of the chamber gas remained at  $-18^{\circ}\text{C}$  within  $\pm 1^{\circ}\text{C}$ .

### 3.2 Three-dimensional Images (Figure 6)

This compares a micro-CT image of a coronary vessel segment harvested from an open-chested, anesthetized pig, during selective injection of 10 mL/4 seconds nonionic (iohexol) contrast agent into the lumen. Note the contrast in the lumen, a vasa vasorum is clearly visible and that the avascular media (smooth muscle layer) and intima are not opacified.

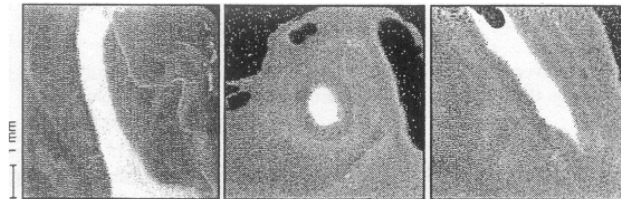


Figure 6 - Micro-CT tomographic images of a frozen porcine coronary obtained during a 2 second injection of intravascular contrast agent. Left panel is a computer-generated projection of the entire specimen. It shows the dye (still) in the main arterial lumen, as well as a very small diameter vasa vasorum on its left. The middle panel is an image of a longitudinal section, and the right panel is an image of a transverse section, through the vessel. Note the lack of opacification of the annular media and intima, but opacification in the adventitia of the vessel wall.

### 3.2.1 Mouse Lung (Figure 7)

This shows one slice of the lung which was scanned in its entirety. The alveoli and airways are clearly air-filled and the blood vessels blood-filled.

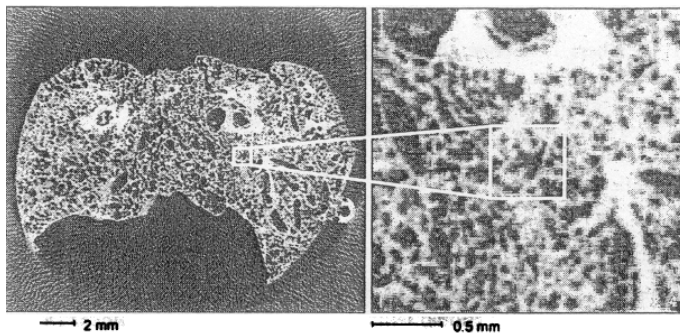


Figure 7 – CT image of a 20 µm thick slice through a mouse lung inflated in situ at 5 mmHg pressure. The right image is a X4 magnification of the left image.

## 4. DISCUSSION

These results demonstrate that it is possible to maintain a frozen specimen at a constant temperature for an extended period of time within a radiolucent container without frost or condensation build up. As we operate the scanner at ~25 keV x-ray photon energy, the attenuation coefficient of water  $\approx 0.9 \text{ cm}^{-1}$ . Hence, 0.1 mm of condensation would reduce the local signal by ~1%. Consequently, any progressive condensation during the scanning process would rapidly invalidate the scan data sets. In addition, these results indicate that this capability allows for rather prolonged x-ray micro-CT scanning of transient events, which last only a few seconds in vivo, at spatial resolution sufficient for visualization of transiently opacified structures the size of vasa vasorum, i.e., 50-100 µm diameter. Moreover, the sharpness of the vascular CT images suggest that no migration of the dye occurs during the post-harvest freezing period.

This approach should, in principle, be applicable to synchrotron-based micro-CT.<sup>3</sup> Even with this intense source of radiation, it is unlikely that the radiation damage and heating are sufficient to significantly alter/thaw the local microstructure of a frozen specimen.<sup>14</sup>

## ACKNOWLEDGEMENTS

This research was supported in part by NIH grant RR11800.

The authors would like to thank Dr. Birgit Kantor for use of her data in Figure 6, Ms. Patricia E. Lund for her technical assistance with the experiments and Ms. Julie M. Patterson who made the illustrations. Ms. Delories C. Darling typed and processed this manuscript.

## REFERENCES

1. F. Peyrin, M. Salome, P. Cloetens, A. M. Laval-Jeantet, E. L. Ritman, and P. Rueggsegger, "Micro-CT examinations of trabecular bone samples at different resolution: 14, 7 and 2 micron level," *Technol. Health Care* **6**, pp. 391-401, 1998.
2. A. Lerman and E. L. Ritman, "Evaluation of microvascular anatomy by micro-CT," *Herz* **24**, pp. 531-533, 1999.
3. R. A. Brooks and G. DiChiro, "Statistical limitations in x-ray reconstruction tomography," *Med. Phys.* **3**, pp. 237-240, 1976.
4. L. Grodzins, "Optimal energies for x-ray transmission tomography of small sample," *Nuc.l Instr. Methods* **206**, pp. 541-545, 1983.
5. S. M. Jorgensen, O. Demirkaya, and E. L. Ritman, "Three dimensional imaging of vasculature and parenchyma in intact rodent organs with x-ray micro-C," *Am. J. Physiol.* **275**(Heart, Circ Physiol **44**), pp. H1103-H1114, 1998.

6. E. L. Ritman, J. H. Dunsmuir, A. Faridani, D. V. Finch, K. T. Smith, and P. J. Thomas, "Local reconstruction applied to x-ray microtomography. IN: Chavent G, Papanicolaou G, Sacks P, Symes W (eds.): *IMA Volumes in Mathematics and Its Applications, Inverse Problems in Wave Propagation* 90, pp. 443-452, Springer-Verlag, New York, 1997.
7. T. A. Giorgi, "Getters and gettering," *Japan J. Appl. Phys. Suppl* 2, Pt 1, pp. 53-60, 1974.
8. C. Crone C, "The permeability of capillaries in various organs as determined by the case of the 'indicator diffusion' method," *Acta Physiol. Scan.* 58, pp. 292-305, 1963.
9. R. E. Brennan, J. A. Curtiss, H. M. Pollack, and I. Weinberg I, " Sequential changes in the CT numbers of the normal canine kidney following intravenous contrast administration II: the renal medulla," *Invest. Radiol.* 14, pp. 239-245, 1979.
10. A. Bergman, A. Magnusson, and A. Sundin, "Relationship between contrast enhancement and diagnostic accuracy with the liver-specific CT contrast medium FP 736-04 in an experimental model of liver metastases," *Acad. Radiol.* 4, pp. 736-741, 1997.
11. L. A. Feldkamp, L. C. Davis, and J. W. Kress, "Practical cone-beam algorithm," *J. Opt. Soc. Am. A.* 1, pp. 612-619, 1984.
12. R. A. Robb, P. B. Heffernan, J. J. Camp, and D. P. Hanson, "A workstation for multi-dimensional display and analysis of biomedical images," *Comput. Meth. Progr. Biomed.* 25, pp. 169-184, 1997.
13. E. L. Ritman, S. M. Jorgensen, P. E. Lund, P. J. Thomas, J. H. Dunsmuir, J. C. Romero, R. T. Turner, and M. E. Bolander, "Synchrotron-based micro-CT of in situ biological Basic Functional Units and their integration. *Proc. SPIE., Developments in X-Ray Tomography* 3149, pp. 13-24, 1997.
14. E. L. Alpen, "Temperature and Radiation Damage: Radiation Biophysics," 2<sup>nd</sup> Ed, pp 197-220, Academic Press, San Diego, 1998.